Polymer Journal, Vol. 34, No. 8, pp 593—600 (2002)

Crystallization Process in Binary Blends of Poly(ε-caprolactone)-*block*-Polybutadiene Copolymers

Satoshi TANIMOTO, Kazuhiro ITO, Shintaro SASAKI, Hiroki TAKESHITA,* and Shuichi NOJIMA**,†

School of Materials Science, Japan Advanced Institute of Science and Technology (JAIST), Tatsunokuchi, Ishikawa 923–1292, Japan
**Department of Material Science and Technology, Nagaoka University of Technology, Kamitomioka, Nagaoka 940–2188, Japan*
***Department of Polymer Chemistry, Tokyo Institute of Technology, 2-12-1 Ookayama, Meguro-ku, Tokyo 152–8552, Japan*

(Received February 7, 2002; Accepted June 17, 2002)

ABSTRACT: The crystallization process in binary blends of poly(ε-caprolactone)-*block*-polybutadiene (PCL-*b*-PB) copolymers has been investigated by time-resolved small-angle X-Ray scattering with synchrotron radiation (SR-SAXS), where the crystallization of PCL blocks induces a morphological transition both in neat copolymers but the crystallization rate is extremely different between them. The microdomain structure in the melt and the final morphology after crystallization were also measured by conventional SAXS, and the melting behavior of crystallized samples was observed by differential scanning calorimetry (DSC). The binary blend forms a single microdomain structure in the melt over the whole composition range investigated, and the crystallization proceeds with an intermediate rate between those of the constituent PCL-*b*-PB copolymers to result in a single lamellar morphology. The time dependence of SR-SAXS curves is qualitatively similar in features to that for the crystallization of pure PCL-*b*-PB copolymers, suggesting that the crystallization of the blend is substantially controlled by a single crystallization mechanism. The remarkable change in the crystallization rate with composition is ascribed to the difference in the stability of preexisting microdomain structures. The conformation of (longer and shorter) PB blocks in the final lamellar morphology is qualitatively discussed.

KEY WORDS Crystalline-Amorphous Diblock Copolymer / Binary Blend / Crystallization Process / Final Morphology /

It is well known that the crystallization of constituent polymers in polymer blends yields a *lamellar morphology*, an alternating structure consisting of lamellar crystals and amorphous layers, where the non-crystalline components are accommodated in the amorphous layers between lamellar crystals or rejected outside the lamellar morphology depending on the degree of segregation between the components.[1] When two homopolymers are both crystalline, a competitive crystallization may occur in a limited range of temperature to result in a complicated morphology. However, miscible crystalline/crystalline homopolymer blends above their melting temperatures are not common, so that the morphological study of such systems is very limited.[2,3] In particular, the miscible binary system, where both homopolymers crystallize in a same temperature range with extremely different rates, has not been reported so far.

The morphology as well as the crystallization behavior of crystalline-amorphous diblock copolymers has been studied extensively,[4–20] and the lamellar morphology is inevitably formed by the crystallization unless the microdomain structure is sufficiently stable. Therefore, the binary blend of crystalline-amorphous diblocks will be a substitutive system for miscible crystalline/crystalline homopolymer blends with extremely different crystallization rates at a same temperature range. That is, it is possible to change widely the crystallization rate by changing the molecular weight and/or block ratio with keeping the miscibility between constituent copolymers, where miscibility means that the components do not segregate macroscopically but make a single microdomain structure in the melt.[21] The crystallization of these binary blends is reminiscent of *molecular fractionation*, as demonstrated for polyethylene samples with a wide molecular weight distribution.[22–24] That is, the crystallization of PCL blocks in binary copolymer blends has a possibility to bring about the macroscopic segregation into individual domains.

In this study, we investigate the crystallization process in binary blends of poly(ε-caprolactone)-*block*-polybutadiene (PCL-*b*-PB) copolymers by time-resolved small-angle X-Ray scattering with synchrotron radiation (SR-SAXS). The constituent copolymers crystallize in a same temperature range with ex-

†To whom correspondence should be addressed (Phone: +81-3-5734-2132, Fax: +81-3-5734-2888, E-mail: snojima@polymer.titech.ac.jp).

tremely different rates, where each microdomain structure of pure copolymers is not preserved but transformed into the lamellar morphology. The morphologies formed in the blends before and after the crystallization of PCL blocks were investigated by conventional SAXS, and the melting behavior of crystallized blends was observed by differential scanning calorimetry (DSC). To understand the cooperative morphology formation between two diblocks, the conformation of the longer and shorter PB blocks is qualitatively discussed.

EXPERIMENTAL

Samples and Blend Preparation

PCL-*b*-PB copolymers used in this study were synthesized by a successive anionic polymerization under vacuum. Details of the synthesis and purification are described elsewhere.[6, 25, 26] We used two PCL-*b*-PB copolymers, M11 and M30, whose molecular characteristics are as follows; M11 : $M_n = 11 \times 10^3$, $M_w/M_n = 1.15$, PCL : PB (vol.%) = 19 : 81 and M30 : $M_n = 30 \times 10^3$, $M_w/M_n = 1.11$, PCL : PB (vol.%) = 11 : 89. The ratio of total molecular weights, M_{M30}/M_{M11}, is 2.7 and that of PCL molecular weights, $M_{M30,PCL}/M_{M11,PCL}$, is 1.6. It was confirmed in our previous study by SAXS and TEM[27] that the crystallization of PCL blocks both in M11 and M30 brought about the morphological transition from the cylindrical or spherical microdomain to the lamellar morphology. The crystallization of M11 is extremely faster than that of M30 at the same crystallization temperature, for instance, M11 crystallizes completely within 45 min at 25°C while M30 takes more than 3 days to crystallize at 25°C.

The blend samples with various compositions were prepared by the casting method with benzene as a common solvent. The sample was finally heated at *ca.* 60°C under reduced pressure to remove the solvent completely.

DSC Measurements

The melting temperature T_m and the crystallinity of PCL blocks χ_w were measured by Parkin–Elmer Pyris 1 DSC. The sample was first kept at *ca.* 60°C for 30 min, quenched into various crystallization temperatures T_c ranging from 13°C to 25°C, maintained at T_c for a long time to complete the crystallization, and finally heated at a rate of 5°C min^{-1} to get the endothermic peak by the melting of PCL blocks. The melting temperature was defined by the peak temperature of the endothermic curve and χ_w was calculated from the endothermic area ΔH by

$$\chi_w = \Delta H/(\Delta H^\circ \phi_{PCL}) \quad (1)$$

where ϕ_{PCL} is the weight fraction of PCL blocks in the binary blend and ΔH° is the heat of fusion for perfect PCL crystals ($\Delta H^\circ = 135.44$ J g^{-1} [28]).

Small-Angle X-Ray Scattering (SAXS) Measurements

We used two SAXS techniques, conventional SAXS (C-SAXS) and time-resolved SAXS with synchrotron radiation (SR-SAXS), for the static and dynamic measurements, respectively.

The microdomain structure formed in the melt and the lamellar morphology after crystallization were investigated by C-SAXS. Details of the apparatus and the measurement condition are described elsewhere.[29] The time necessary for each C-SAXS measurement was 60 min, and T_c was changed from 9°C to 39°C depending on ϕ_{M11} (weight fraction of M11 in the system). The crystallization process was pursued by SR-SAXS at Institute of Materials Structure Science, Tsukuba Japan (Photon Factory), with small-angle X-Ray equipment for solution (SAXES) installed on beam line BL-10C. Details of the optics and the instrumentation were described elsewhere.[6, 16, 30] The SAXS intensity was collected as an accumulation of the scattered intensity during 10 s and corrected for a minor decrease in the storage ring current during measurements, which was continuously monitored by an ionization chamber placed just before the sample.

The SAXS curves measured by both the methods were corrected for the background scattering and absorption by the sample but not for the smearing effect because the optics employed for both SAXS apparatuses was point focusing. The SAXS curve was finally obtained as a function of s defined by

$$s = 2 \sin\theta/\lambda \quad (2)$$

where 2θ is the scattering angle and λ is the X-Ray wave length (0.1542 nm for C-SAXS and 0.1488 nm for SR-SAXS). There was no discrepancy detected between the data measured by both methods.

Data Analysis of SR-SAXS Results

We focused our attention on the time dependence of the peak intensity I_{max} and peak position s_{max} of SR-SAXS curves arising from the microdomain structure and lamellar morphology. That is, I_{max} and $1/s_{max}$ (*i.e.*, spacing of the structure) were plotted against crystallization time to clarify the difference in the crystallization behavior among blends with different ϕ_{M11} and T_c. For some cases, the angular position of SAXS intensity peaks from the microdomain structure was very close to that from the lamellar morphology to make the evaluation of I_{max} and s_{max} difficult.[16, 31] For such a case, we

approximated each SAXS peak with the Lorentz function,

$$I(s) = \frac{2A}{\pi w}\left\{1 + \frac{4}{w^2}(s - s_{\max})^2\right\}^{-1} \quad (3)$$

where w is the full width at half maximum of the peak and A is proportional to the peak area. This function is usually used to approximate the diffraction intensities from crystalline materials to characterize each peak without any theoretical basis.

RESULTS

Microdomain Structure in the Melt

First of all it is necessary to check whether M11 and M30 are totally miscible or not at the molecular level in the melt. That is, if the two copolymers are miscible they make a single microdomain structure and the average spacing changes continuously with composition.[21] If they are macroscopically segregated, on the other hand, we can observe two microdomain structures, the spacing of which exactly corresponds to those of the constituent copolymers if the shorter block does not dissolve partially in the domain consisting of longer one.[32]

The SAXS intensity curves are logarithmically plotted in Figure 1 for various molten blends (at *ca.* 60°C), in which the angular position of SAXS intensity peaks moves continuously with composition. The domain spacing evaluated from the peak position is plotted in the inset of Figure 1 as a function of ϕ_{M11}. The domain spacing of the blend takes an intermediate value between those of constituent copolymers (M11 and M30) and increases steadily with decreasing ϕ_{M11}, indicating that M11 and M30 do not segregate macroscopically to form individual domains but make cooperatively a single microdomain structure irrespective of ϕ_{M11}. M30 has a cylindrical microdomain structure considering the positions of higher-order diffractions shown in Figure 1. The microdomain structure of M11, on the other hand, cannot be decided from Figure 1 because of the lack of higher-order diffractions, but it is supposed to be spherical judging from the PCL composition in the blend.

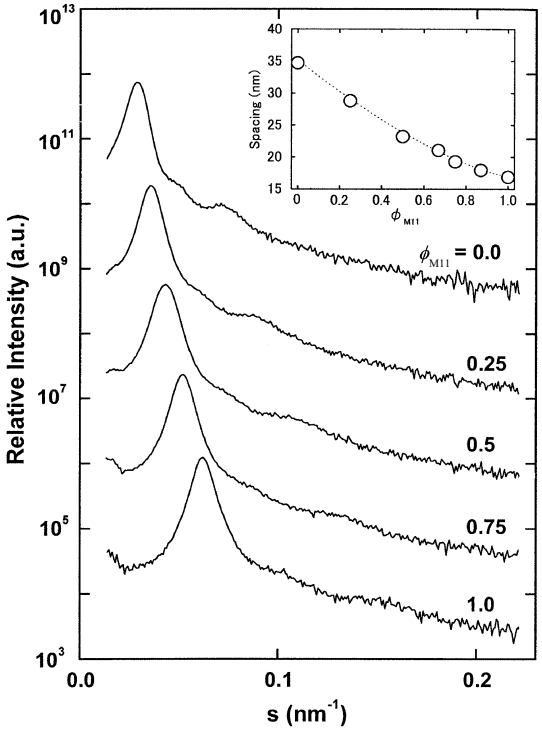

Figure 1. SAXS intensity curves logarithmically plotted against wave number s for various binary blends in the melt (*ca.* 60°C). The inset represents the ϕ_{M11} dependence of the spacing of microdomain structures.

The formation of a single microdomain structure was confirmed experimentally for some binary blends of amorphous-amorphous diblock copolymers.[21,32–35] Hashimoto *et al.*,[21,32] for example, demonstrated that when the constituent copolymers were satisfied with the condition of $M_\alpha/M_\beta < 5$ (where M_α and M_β are the molecular weight of copolymer α and β, respectively), they made a single microdomain structure even if there was a difference in composition between the copolymers. Furthermore they showed that the binary blend of block copolymers with unequal chain length might change the interface curvature of microdomains to result in a morphological transition from the lamella into the bicontinuous structure even if both the constituent copolymers took the lamellar morphology. In the present case, $M_{M30}/M_{M11} \approx 2.7$ and the PCL composition is not so different between M11 and M30, which agree with the criterion proposed by Hashimoto *et al.* on the miscibility between two block copolymers. In summary, we can conclude that M11 and M30 are molecularly miscible to make cooperatively a single microdomain structure in the melt.

Crystallization Behavior

Figure 2 shows the three-dimensional overview of time-resolved SR-SAXS curves for $\phi_{M11} = 1.0$ (a) and 0.5 (b) crystallized at 25°C. The SAXS intensity peak arising from the microdomain structure decreases and simultaneously that from the lamellar morphology increases with crystallization time t. The angular position of these two peaks separates adequately for the case of $\phi_{M11} = 1.0$ and therefore it is easy to evaluate the t dependence of these peaks (*i.e.*, intensity and position). However, the position of intensity peaks for the blend with $\phi_{M11} = 0.5$ is very close with each other and it is necessary to use the computational method to separate them. We applied eq 3 for each peak on SR- SAXS

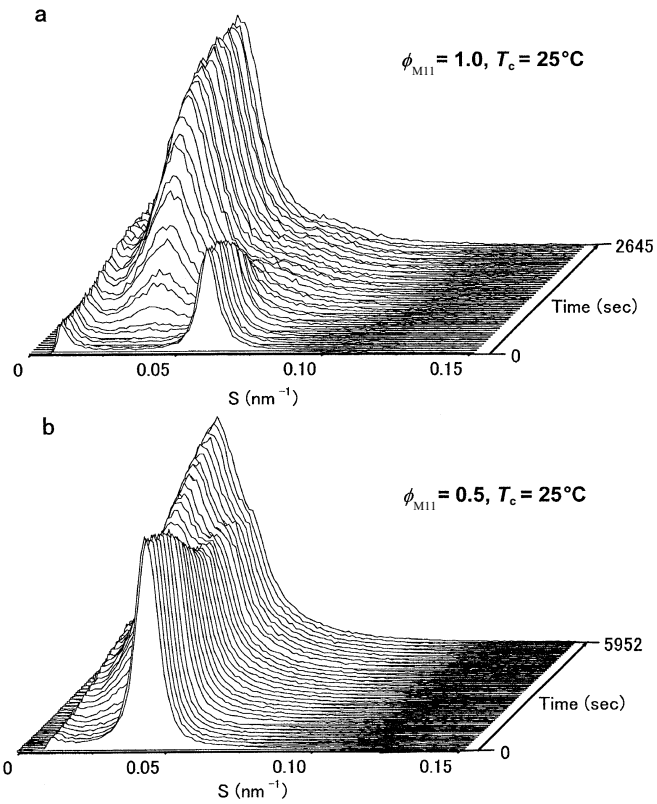

Figure 2. Overview of time-resolved SAXS curves during crystallization at 25°C for (a) ϕ_{M11} = 1.0 and (b) ϕ_{M11} = 0.5.

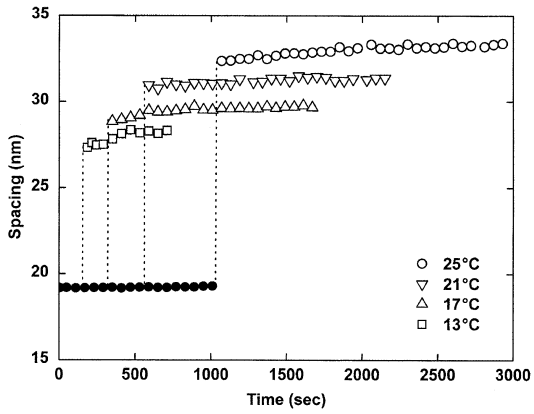

Figure 3. Spacing, evaluated from the angular position of the SAXS intensity maximum, plotted against crystallization time for ϕ_{M11} = 0.75 crystallized at various temperatures indicated. The closed symbol represents the spacing of microdomain structure and the open symbols those of lamellar morphology.

curves during crystallization.

Figure 3 shows the t dependence of the major spacing for the blend with ϕ_{M11} = 0.75 at various crystallization temperatures T_c indicated. The major spacing corresponds to the highest peak at t when each peak is normalized, *i.e.*, when each peak is divided by the initial (for the case of scattering from the microdomain structure) or the final (from the lamellar morphology) peak intensity. The spacing of the microdomain structure (closed circle in Figure 3) is constant irrespective

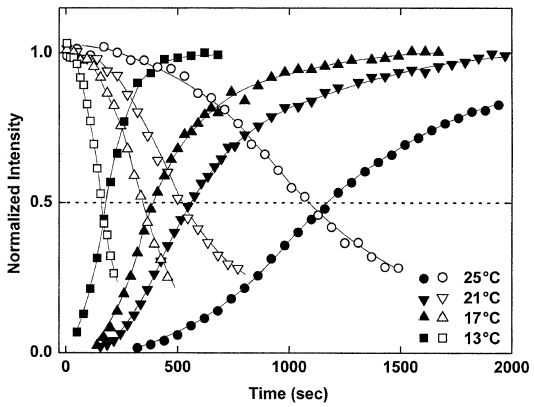

Figure 4. Normalized peak intensity plotted against crystallization time for the blend with ϕ_{M11} = 0.75 crystallized at various temperatures indicated. The open symbols represent the scattering intensities from the microdomain structure and the closed symbols those from the lamellar morphology.

of T_c, and it turns suddenly into a larger spacing that reflects the formation of lamellar morphology in the system. The spacing of this lamellar morphology increases significantly with increasing T_c, as usually observed in homopolymer crystallization.

Figure 4 shows the t dependence of the normalized peak intensity for the blend with ϕ_{M11} = 0.75 crystallized at various T_c indicated. The normalized intensity from the microdomain structure (open symbols) decreases with an inverse sigmoidal shape, whereas that from the lamellar morphology (closed symbols) increases with a sigmoidal shape, and they coincide with each other when both normalized intensities equal approximately to 0.5. This fact indicates that the morphological transition occurs directly from the microdomain structure into the lamellar morphology without forming any third phase (for example, disordered phase), as pointed out in our previous study.[6] The sigmoidal increase of the peak intensity is usually observed during the crystallization of homopolymers and polymer blend systems,[36,37] which indicates the Avrami-type crystal growth. In fact, the Avrami analysis using the scattering intensity as shown in our previous study[25] gives the Avrami exponent n ranging from 2 to 3, suggesting two-dimensional (n = 2) or three-dimensional (n = 3) growth with heterogeneous nucleation. The value of n obtained is indistinguishable from that widely reported for typical crystalline homopolymers such as high density polyethylene[38] and poly(ethylene oxide),[39] which indicates that the existing microdomain structure does not affect the subsequent crystallization. In addition, it is found from Figure 4 that the crystallization is prolonged considerably with increasing T_c, which we already reported for the crystallization of PCL-*b*-PB copolymers[26] and PCL homopolymers in the binary blend with polystyrene oligomers.[30]

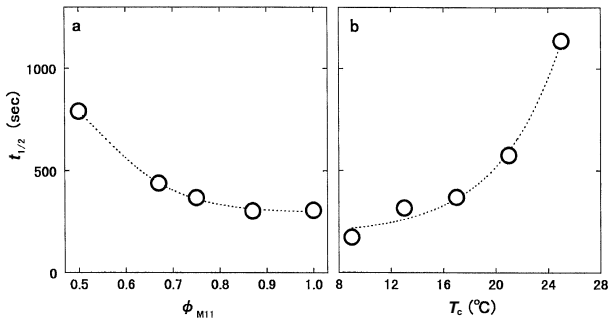

Figure 5. Half time necessary to reach the final value at the angular position of the intensity maximum, $t_{1/2}$, plotted against ϕ_{M11} at $T_c = 17°C$ (a) and against T_c for the blend with $\phi_{M11} = 0.75$ (b).

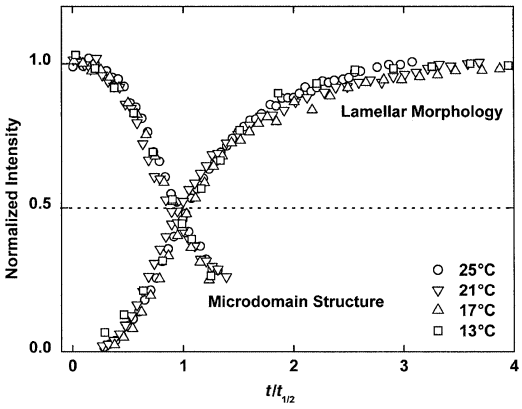

Figure 6. Normalized peak intensity, arising from the lamellar morphology and microdomain structure, plotted against reduced time $t/t_{1/2}$ for $\phi_{M11} = 0.75$.

It is possible to calculate the half time of crystallization $t_{1/2}$, that is, the time necessary to reach half of the final peak intensity due to the crystallization, which equals approximately to the time necessary to reach half of the initial peak intensity arising from the microdomain structure because both the normalized intensities meet roughly at their half values. Figure 5 shows the ϕ_{M11} dependence of $t_{1/2}$ for $T_c = 17°C$ (a) and T_c dependence of $t_{1/2}$ for $\phi_{M11} = 0.75$. $t_{1/2}$ increases remarkably with decreasing ϕ_{M11} and increasing T_c, suggesting that blending M30, which has a much slow crystallization rate compared to that of M11, has the significant effect of decreasing the crystallization rate similar to increasing T_c. We can find from Figures 3–5 that M11 and M30 do not crystallize separately to yield individually crystallized regions but take a cooperative crystallization over the whole ϕ_{M11} and T_c to result in a single lamellar morphology. This is the most important experimental result in this study, though it is counterintuitive when considering the crystallization fractionation sometimes observed in crystalline homopolymers.[22–24]

To investigate the details of the crystallization behavior, the normalized intensities are plotted in Figure 6 against reduced crystallization time $t/t_{1/2}$, *i.e.*, the crystallization time divided by the half time of crystallization, for $\phi_{M11} = 0.75$ at various T_c indicated. Although the time dependence of the peak intensities from the microdomain structure and lamellar morphology shows different curves (Figure 4) according to T_c, they coincide with each other and make one master curve in Figure 6. The normalized intensities for different ϕ_{M11} but a same T_c show the similar results. This means that the morphology reorganization from the microdomain structure into the lamellar morphology in our binary copolymer systems is controlled by a single crystallization mechanism that is qualitatively similar to that of the constituent block copolymers, and the crystallization proceeds with one crystallization rate between those of neat copolymers. As a result, we have a single lamellar morphology uniformly composed of two PCL-*b*-PB copolymers, in which we can expect an interesting *compromise* between longer and shorter PCL-*b*-PB copolymers.

Lamellar Morphology after Crystallization

In our previous study by SAXS and TEM,[27] both M11 and M30 formed the lamellar morphology after the crystallization of PCL blocks, and therefore the lamellar morphology is naturally expected for the crystallized blends composed of M11 and M30. Details of this morphology can be evaluated quantitatively from the DSC and SAXS results. That is, the lamella thickness ℓ_c and the amorphous layer thickness ℓ_a (which consists of the amorphous PCL layer $\ell_{PCL,a}$ and PB layer ℓ_{PB}) are calculated by

$$\ell_c = L\chi_v \tag{4}$$

$$\ell_a = \ell_{PCL,a} + \ell_{PB} = L(1 - \chi_v) \tag{5}$$

where L is the long spacing obtained by the SAXS measurement and χ_v is the volume fraction of crystallized PCL blocks against the total sample.

Figure 7 shows the ϕ_{M11} dependence of L (a) and ℓ_c and ℓ_{PB} (b) at various T_c indicated. The value of ℓ_c is about 3 nm irrespective of ϕ_{M11} and T_c, which is somewhat smaller than the lamella thickness observed in crystalline homopolymers (5–10 nm for PCL and *iso*-polystyrene in miscible binary blends[1]). The thin lamella is often observed in the morphology formed in crystalline-amorphous diblock copolymers with small crystalline blocks. Mai *et al.*,[40] for example, obtained the lamellar morphology with extremely thin lamellae (3–4 nm thick) for quenched poly(ethylene oxide)-*block*-poly(butylene oxide) copolymers. The 3 nm lamella thickness obtained in the present study is a foregone conclusion originating from the assumption of lamellar morphology for the crystallized blends, which

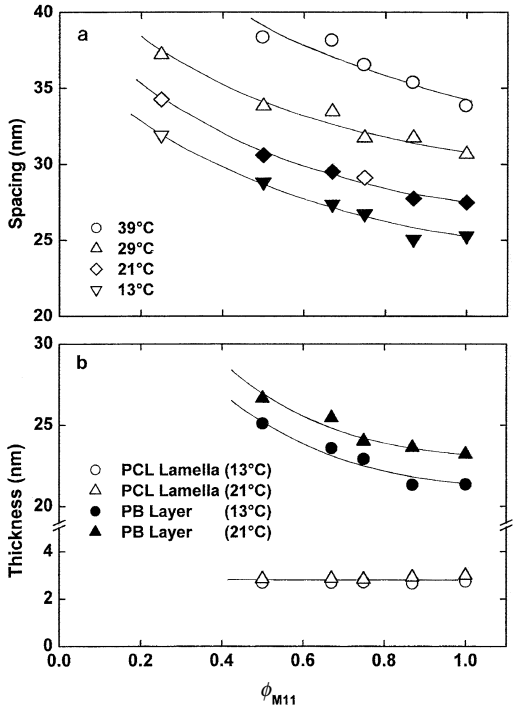

Figure 7. (a) Long spacing for alternating structure consisting of PCL lamellae and PCL+PB amorphous layers and (b) PCL lamella thickness (open symbols) and PB layer thickness (closed symbols) plotted against ϕ_{M11}. The closed symbols in (a) were obtained by SR-SAXS method and open ones by C-SAXS method.

seems reasonable considering that pure M11 and M30 form the respective lamellar morphology after the crystallization of PCL blocks. If we assume that the two PCL blocks make cooperatively a lamellar crystal with 3 nm in thickness, the folding number of the shorter PCL block (M11) is 2.5–3 and that of the longer one (M30) is 5–6 (depending on the crystallinity).

Figure 7 indicates clearly that the increase of L with decreasing ϕ_{M11} comes from the increase of the PB layer thickness, which arises simply from the increase in the proportion of bulky PB blocks belonging to M30.

DISCUSSION

Crystallization Rate

It is known that the crystallization of homopolymers is controlled by two factors; (1) the dynamic factor related to the activated energy for the transport of crystalline units across the phase and (2) the static factor associated with the free energy barrier for nucleation. These two factors restrict the crystallization within the temperature range between T_g and T_m, and the maximum crystallization rate lies in the middle of the two temperatures. The molecular weight dependence of crystallization rate has been investigated extensively for many crystalline homopolymers,[41] where the molecular weight mainly influences the rate through the dynamic factor mentioned above. Maclaine and Booth,[42,43] for example, investigated the crystallization rate for various poly(ethylene oxide) fractions ranging in molecular weight M from 10^4 to 10^6 by dilatometric methods and spherulite observations, and found that the crystallization rate did not decrease but increased with increasing M in the low molecular weight range ($M < 50000$). This fact was verified for polyethylene (PE), where the spherulite growth rate for various PE fractions ($3900 < M < 87000$) increased with increasing M when compared at constant T_c.[44] In the present case, the total crystallization rate of M30 is extremely slower than that of M11; $t_{1/2}$ of M11 at $T_c = 21°C$ is about 600 s, while that of M30 at $T_c = 21°C$ is over 24 h. Here, $M_{M30,PCL}/M_{M11,PCL}$ is only 1.6 (and also $M_{M30}/M_{M11} \approx 2.7$) and the absolute molecular weight of both M11 and M30 is relatively small compared to the homopolymers usually used for the dynamic study of crystallization. These facts suggest that the dynamic factor does not affect dominantly the pronounced difference in the crystallization rate between M11 and M30.

The stability of microdomain structures in the melt has to be included when we consider the static factor for the crystallization of block copolymers. That is, the microdomain structure of higher molecular weight copolymers is more stable, giving the higher energy barrier for nucleation to yield the slower crystallization rate. For the present binary blend of M11 and M30, a single microdomain structure is cooperatively formed and the stability of this structure will be intermediate between those of the constituent copolymers and strongly dependent on ϕ_{M11}. Therefore it is reasonable to consider that the preexisting microdomain structure controls the total crystallization rate through the extra energy barrier generated by the formation of this structure. In conclusion, we can say that the dramatic change in the crystallization rate against ϕ_{M11} is characteristic of block copolymer blends. That is, such a change is not expected for the binary blend of crystalline homopolymers because changing the stability of the homogeneous melt is not expected with changing composition.

Conformation of PB Blocks in the Lamellar Morphology

It is interesting to examine the conformational compromise between the longer and shorter PB blocks in a single lamellar morphology. We can suppose two possible models for the conformation of both the PB blocks in the amorphous layer, as schematically depicted in Figure 8. Figure 8a shows that both blocks together make a homogeneous amorphous layer to fill

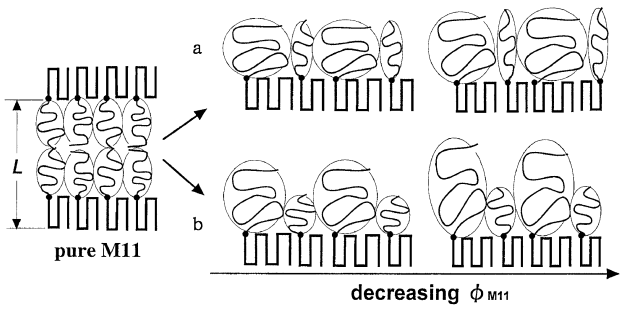

Figure 8. Schematic illustration showing the ϕ_{M11} dependence of the PB block conformation in the lamellar morphology. In (a) and (b) upper PB blocks are omitted for clarity. The circles stand for chain dimensions.

the space uniformly and consequently the shorter block has to be stretched to the direction normal to the lamella surface. It is found by using the same calculation presented in our previous study[16] that the PB block in pure M11 is slightly elongated in the direction perpendicular to the interface, which is consistent with the theoretical predictions.[45, 46] The degree of elongation for the shorter PB block (belonging to M11) increases steadily with decreasing ϕ_{M11} and eventually it reaches the size 1.6 times larger than that of unperturbed dimension at $\phi_{M11} \approx 0.5$. In addition, at the limit of $\phi_{M11} \rightarrow 0$ an unrealistic elongation of the shorter PB block and therefore an extremely large elastic energy are suggested if we keep the situation shown in Figure 8a. Therefore we will have to consider the change in the interface curvature between lamellar crystals and amorphous layers as suggested by Hashimoto *et al.* for the binary blend of symmetrical amorphous-amorphous diblock copolymers,[21] or the localization of the shorter PB block in the lamellar morphology (Figure 8b), as suggested by Sakurai *et al.* for the microdomain structure consisting of shorter and longer amorphous-amorphous diblock copolymers.[35] We can easily suppose for the former case that the lamellar crystal is hard to change the interface curvature to accommodate both the longer and shorter PB blocks in the amorphous layer. In the latter case the PB blocks do not distribute uniformly in the amorphous layer, but the middle of amorphous layers consists of the longer PB block and the interface mainly consists of the shorter PB block. Unfortunately it is now impossible from the present data to independently estimate the shape of the longer and shorter PB blocks in the amorphous layer.

CONCLUSIONS

The crystallization behavior and resulting morphology of binary blends of PCL-*b*-PB diblock copolymers were studied as a function of composition by SR-SAXS, C-SAXS, and DSC, where the crystallization rate of pure copolymers was extremely different. The binary blend made a single microdomain structure in the melt over the whole composition range. The crystallization proceeded with an intermediate rate between those of the constituent copolymers to result in a single lamellar morphology, indicating that the crystallization of this binary blend is driven by a single crystallization mechanism as in the case of pure PCL-*b*-PB copolymers. The steep change in the total crystallization rate with ϕ_{M11} will be ascribed to the difference in the stability of preexisting microdomain structures, because many studies on the molecular weight dependence of homopolymer crystallization show that the dynamic factor does not contribute to the dramatic decrease of the rate in this molecular weight range. The final morphology was qualitatively discussed by assuming a single lamellar morphology uniformly consisting of M11 and M30 (Figure 8a). The degree of deformation for the shorter PB block increased with decreasing ϕ_{M11}, and eventually at the limit of $\phi_{M11} \rightarrow 0$ an unrealistic elongation of the shorter PB block was suggested, for which an alternate model (Figure 8b) was suggested.

Acknowledgment. This work was supported in part by Grants-in-Aid for Scientific Research on Basic Areas (C) (No. 12650879) and on Priority Areas (A), "Dynamic Control of Strongly Correlated Soft Materials" (No. 413/13031035) from the Ministry of Education, Culture, Sports, Science and Technology of Japan and has been performed under the approval of the Photon Factory Advisory Committee (Nos. 99G053 and 99G264).

REFERENCES

1. R. S. Stein, F. B. Khambatta, F. P. Warner, T. Russell, A. Escala, and J. Balizer, *J. Polym. Sci., Polym. Symp.*, **63**, 313 (1978).
2. M. Ree, T. Kyu, and R. S. Stein, *J. Polym. Sci., Part A: Polym. Chem.*, **25**, 105 (1987).
3. J. C. Lee, H. Tazawa, T. Ikehara, and T. Nishi, *Polym. J.*, **30**, 780 (1998).
4. I. W. Hamley, "The Physics of Block Copolymers", Oxford University Press, Oxford, London, 1998.
5. S. Ishikawa, K. Ishizu, and T. Fukutomi, *Polym. Commun.*, **32**, 374 (1991).
6. S. Nojima, K. Kato, S. Yamamoto, and T. Ashida, *Macromolecules*, **25**, 2237 (1992).
7. K. C. Douzinas and R. E. Cohen, *Macromolecules*, **25**, 5030 (1992).
8. P. Rangarajan, R. A. Register, and L. J. Fetters, *Macromolecules*, **26**, 4640 (1993).

9. K. Sakurai, W. J. MacKnight, D. J. Lohse, D. N. Schulz, and J. A. Sissano, *Macromolecules*, **27**, 4941 (1994).
10. L. Liu, B. Jiang, and E. Zhou, *Polymer*, **37**, 3937 (1996).
11. V. Balsamo, F. Gyldenfeldt, and R. Stadler, *Macromol. Chem. Phys.*, **197**, 3317 (1996).
12. L. Z. Liu, F. Yeh, and B. Chu, *Macromolecules*, **29**, 5336 (1996).
13. I. W. Hamley, J. P. A. Fairclough, N. J. Terrill, A. J. Ryan, P. M. Lipic, F. S. Bates, and E. T. Andrews, *Macromolecules*, **29**, 8835 (1996).
14. G. Floudas and C. Tsitsilianis, *Macromolecules*, **30**, 4381 (1997).
15. B. Bogdanov, A. Vidts, E. Schacht, and H. Berghmans, *Macromolecules*, **32**, 726 (1999).
16. S. Nojima, N. Kikuchi, A. Rohadi, S. Tanimoto, and S. Sasaki, *Macromolecules*, **32**, 3727 (1999).
17. Y. L. Loo, R. A. Register, and A. J. Ryan, *Phys. Rev. Lett.*, **84**, 4120 (2000).
18. T. Shiomi, H. Tsukada, H. Takeshita, K. Takenaka, and Y. Tezuka, *Polymer*, **42**, 4997 (2001).
19. L. Zhu, S. Z. D. Cheng, B. H. Calhoun, Q. Ge, R. P. Quirk, E. L. Thomas, B. S. Hsiao, F. Yeh, and B. Lotz, *Polymer*, **42**, 5829 (2001).
20. S. Hong, W. J. MacKnight, T. P. Russell, and S. P. Gido, *Macromolecules*, **34**, 2876 (2001).
21. T. Hashimoto, K. Yamasaki, S. Koizumi, and H. Hasegawa, *Macromolecules*, **26**, 2895 (1993).
22. J. L. Kardos, H. M. Li, and K. A. Huckshold, *J. Polym. Sci., A-2*, **9**, 2061 (1971).
23. A. Mehta and B. Wunderlich, *Makromol. Chem.*, **153**, 327 (1972).
24. A. Mehta and B. Wunderlich, *Colloid Polym. Sci.*, **253**, 193 (1975).
25. S. Nojima, H. Nakano, Y. Takahashi, and T. Ashida, *Polymer*, **35**, 3479 (1994).
26. S. Nojima, S. Yamamoto, and T. Ashida, *Polym. J.*, **27**, 673 (1995).
27. A. Rohadi, R. Endo, S. Tanimoto, S. Sasaki, and S. Nojima, *Polym. J.*, **32**, 602 (2000).
28. V. Crescenzi, G. Manzini, G. Calzolari, and C. Borri, *Eur. Polym. J.*, **8**, 449 (1972).
29. S. Nojima, K. Hashizume, A. Rohadi, and S. Sasaki, *Polymer*, **38**, 2711 (1997).
30. S. Nojima, K. Kato, M. Ono, and T. Ashida, *Macromolecules*, **25**, 1922 (1992).
31. S. Nojima, Y. Kanda, and S. Sasaki, *Polym. J.*, **30**, 628 (1998).
32. T. Hashimoto, S. Koizumi, and H. Hasegawa, *Macromolecules*, **27**, 1562 (1994).
33. S. Koizumi, H. Hasegawa, and T. Hashimoto, *Macromolecules*, **27**, 4371 (1994).
34. J. Zhao, B. Majumdar, M. F. Schulz, F. S. Bates, K. Almdal, K. Mortensen, D. A. Hajduk, and S. M. Gruner, *Macromolecules*, **29**, 1204 (1996).
35. S. Sakurai, H. Umeda, A. Yoshida, and S. Nomura, *Macromolecules*, **30**, 7614 (1997).
36. B. S. Hsiao, K. H. Gardner, D. Q. Wu, and B. Chu, *Polymer*, **34**, 3986 (1993).
37. R. K. Verma, V. Velikov, R. G. Kander, H. Marand, B. Chu, and B. S. Hsiao, *Polymer*, **37**, 5357 (1996).
38. D. M. Hoffman and B. M. Mckinley, *Polym. Eng. Sci.*, **25**, 562 (1985).
39. Y. K. Godovsky, G. L. Slonimsky, and N. M. Garbar, *J. Polym. Sci., C*, **38**, 1 (1972).
40. S. M. Mai, J. P. A. Fairclough, K. Viras, P. A. Gorry, I. W. Hamley, A. J. Ryan, and C. Booth, *Macromolecules*, **30**, 8392 (1997).
41. B. Wunderlich, "Macromolecular Physics Vol. 1," Academic Press, Inc., New York, N.Y., 1973.
42. J. Q. G. Maclaine and C. Booth, *Polymer*, **16**, 191 (1975).
43. J. Q. G. Maclaine and C. Booth, *Polymer*, **16**, 680 (1975).
44. P. H. Lindenmeyer and V. F. Holland, *J. Appl. Phys.*, **35**, 55 (1963).
45. E. A. DiMarzio, C. A. Guttman, and J. D. Hoffmann, *Macromolecules*, **13**, 1194 (1980).
46. M. D. Whitmore and J. Noolandi, *Macromolecules*, **21**, 1482 (1988).